

Hairpins with Poly-C Loops Stabilize Four Types of Fluorescent Ag_n:DNA

Patrick R. O'Neill,^{*,†} Lourdes R. Velazquez,[†] Donald G. Dunn,[‡] Elisabeth G. Gwinn,[†] and D. Kuchnir Fygenson[†]

Physics Department, Mail Code 9530, Chemistry and Biochemistry Department, Mail Code 9510, and Biomolecular Science and Engineering Program, University of California, Santa Barbara, Santa Barbara, California 93106-9530

Received: October 20, 2008; Revised Manuscript Received: February 10, 2009

Few-atom Ag clusters self-assemble on single-stranded DNA and exhibit sequence-dependent fluorescence ranging from the blue to the NIR. DNA sequence presents a very large parameter space for creating new Ag_n:DNA emitters, with potential for improved fluorescence and chemical stability. Exploration of this parameter space may be greatly facilitated by the identification of classes of emitters that share similar features, helping provide insight into their fluorescence-determining physical features. We synthesize Ag clusters on DNA hairpins with 3 to 12 cytosines (C's) in the loop, and observe loop-dependent fluorescence. All of these hairpins support fluorescence, and all but the smallest yield more than one spectral peak. The 19 fluorescence peaks fall into four groups based on their wavelengths and chemical stability. Correlations between fluorescence and mass spectroscopy of the 9C hairpin emitters link Ag₁₁:DNA with green fluorescence and Ag₁₃:DNA with red fluorescence.

Introduction

Few-atom noble-metal clusters are smaller than plasmon-supporting metallic nanoparticles and exhibit electronic transitions within the conduction band that produce visible fluorescence.¹ Fluorescent Ag nanoclusters can be stabilized in aqueous solution using DNA.² They are especially interesting for their photophysical properties³ and because they self-assemble directly on single-stranded DNA with sequence dependent fluorescence.⁴ Given recent developments in DNA self-assembly that enable high-yield production of 100-nm-square DNA grids with unique 6 nm pixels,⁵ one of the most exciting applications of Ag nanoclusters would be as optically addressable quantum systems that can be positioned with nanoscale precision and without coupling chemistries using DNA nanotechnology.⁶ Site-specific self-assembly of fluorescent Ag clusters on such DNA grids would enable rational design of short-range optical interactions⁷ with potentially important implications for information processing.⁸

Fluorescent Ag clusters have been studied in rare gas matrices⁹ and zeolites¹⁰ since the early 1980s. Recently, Dickson and colleagues have shown that they can also exist in aqueous solution, stabilized by dendrimers,¹¹ peptides,¹² or DNA oligomers.² As yet, very little is known about the detailed structure of DNA-bound Ag clusters and how it influences optical properties.

Systematic variation of the host DNA sequence and structure, combined with spectroscopic studies, can uncover fundamental properties of Ag_n:DNA emitters. Experiments until now have emphasized the influence of DNA sequence on Ag cluster fluorescence. A large random sampling of 12 base DNA

sequences yielded emitters ranging from the blue to the near-infrared.¹³ Sequence modifications of DNA hairpins with homopolymeric 5-base loops revealed that C's and G's stabilize fluorescent clusters best.⁴ Here we expand on these hairpin studies using DNA hairpins with all-C loops, and show that the number of C's in the loop tunes Ag cluster stability and fluorescence.

Experimental Methods

Our DNA sequences are predicted to form hairpins with 7 base-pair stems and single stranded loops of 3 to 12 cytosines (TATCCGT-C_n-ACGGATA, with $n = 3$ to 12).¹⁴ To make fluorescent Ag nanoclusters, we mix AgNO₃ with DNA in ammonium acetate, age the mixtures at 4 °C for 1 h, reduce them with NaBH₄ and store them at 4 °C. Unlike most cations, Ag⁺ ions bind exclusively to DNA bases, not to the negatively charged phosphates of the DNA backbone.¹⁵ Chemical reduction of Ag⁺ ions causes the formation of silver clusters that can grow into large aggregates. DNA both nucleates and limits cluster growth. Single-stranded and double-stranded DNA bind Ag⁺ ions, but only single-stranded DNA has the conformational flexibility to stabilize visibly fluorescent clusters.⁴

The final mixtures contain 40 mM ammonium acetate, 25 μM DNA, 150 μM AgNO₃, and 50 μM NaBH₄. We use ammonium acetate for its compatibility with electrospray ionization (ESI) mass spectroscopy. The Ag:DNA ratio (6:1) follows that of previous protocols.^{2,4} Notably, we use a lower ratio of BH₄⁻:Ag⁺ than previous protocols (1:3 as compared to 1:1² or even 2:1⁴). We find this leads to a faster onset of fluorescence and in many cases a brighter maximum intensity, although it also results in shorter chemical lifetimes for some emitters. We have synthesized emitters on the 9C hairpin more than 20 times, and on the 6C, 7C, and 12C hairpins more than

* Corresponding author. E-mail: patrick@physics.ucsb.edu.

[†] Physics Department.

[‡] Chemistry and Biochemistry Department.

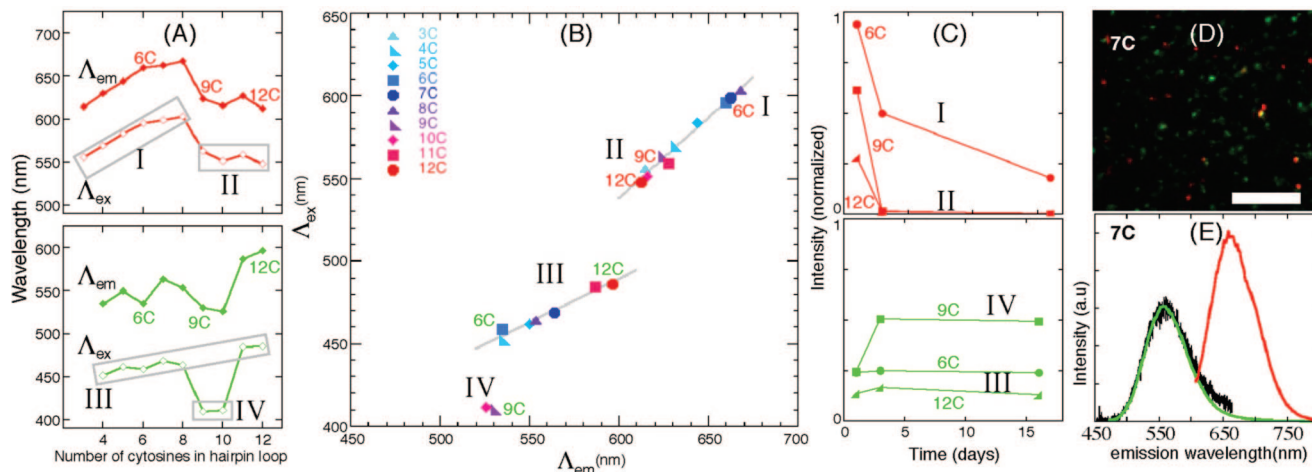


Figure 2. The 19 fluorescence peaks fall into four groups on the basis of (A) wavelength dependence on the number of cytosines in the hairpin loop, (B) excitation vs emission wavelengths, and (C) time-dependent intensities (normalized to the brightest (6C) red) peak. The different time-dependence of red and green peaks in (C) suggests there are distinct red and green emitters rather than a single species with two radiative transitions. Fluorescence microscopy of 7C clusters spin cast in PVA supports this conclusion (D). The corresponding solution fluorescence is shown in (E) (red and green curves), along with the ensemble green emission of PVA embedded clusters (black curve). Scale bar: 10 μm .

fluorescence properties of the clusters in solution are not significantly perturbed in PVA.

The organization of emitters into four groups raises two important questions. What physical features make emitters in one group different from those in another, and what physical changes are responsible for the small spectral shifts within a group of emitters?

In addressing these questions, many aspects of emitter composition and structure warrant consideration. Symmetry is key in determining which electronic transitions are optically allowed, so cluster geometry must influence fluorescence. Cluster charge likely also plays a role, as indicated by theoretical absorption spectra, which differ for neutral and cationic Ag clusters.¹⁸ Furthermore, time-dependent density functional theory calculations (performed without solvent) suggest that binding to the ring nitrogen of pyridine can dramatically change the absorbance spectra of Ag clusters.¹⁹ Binding to DNA bases may thus also play an important role in determining the optical properties of the clusters. Finally, fluorescent spectra of Ag clusters in argon matrices indicate that transition energies depend strongly on the number of atoms in the cluster, but do not exhibit any simple scaling law.^{20–23} We therefore anticipate that $\text{Ag}_n\text{:DNA}$ fluorescence depends strongly on n , the number of Ag atoms in the cluster.

From a practical point of view, n is also the simplest of these features to assess. We set out to determine the composition of emitters from two different groups by mass spectroscopy. We focused on the 9C hairpin, because the strong (and opposite) time dependence of its two fluorescence peaks facilitates the search for correlations between fluorescence intensity and mass abundance of various $\text{Ag}_n\text{:DNA}$ species. We synthesized clusters in 40 mM ammonium acetate, using 25 μM DNA, 150 μM AgNO_3 , and 50 μM NaBH_4 . We stored the solution at 4 $^\circ\text{C}$, and froze (-80 $^\circ\text{C}$) aliquots various times after reduction (5 min, 30 min, 1 h, 5 h, and 1 day), taking two aliquots at each time point: one for fluorescence and one for mass spectroscopy. Between 5 h and 1 day, the solution was kept at room temperature instead of 4 $^\circ\text{C}$ to speed up the conversion of red to green. One day after reduction, an additional 50 μM NaBH_4 was added, and again aliquots were frozen at various times after this second reduction (5 min, 30 min, 5 h). One day after freezing the final aliquots, we thawed each aliquot and im-

mediately measured its fluorescence in turn (emission scans for excitation from 280 to 700 nm in 20 nm steps). Later that day, we thawed each duplicate aliquot and immediately measured its mass spectrum in turn.

Excitation of these solutions at 560 nm produced red fluorescence peaked at 620 nm, with a spectrum identical in all 8 samples, suggesting that it can be assigned to a single cluster type (Supporting Information). Excitation at 400 nm produced the same green fluorescence spectrum, peaked at 526 nm in all 8 samples, with the exception that in samples with high intensities of red fluorescence (560 nm, 620 nm), the green spectrum had a small secondary maximum at 620 nm, perhaps indicating FRET between nearby green and red clusters (Supporting Information). Like red, green (400 nm, 526 nm) intensity most likely corresponds to fluorescence from a single cluster type.

Red fluorescence was most intense 5 min after the initial reduction and least intense 1 day after reduction (Supporting Information). Conversely, the green fluorescence was least intense 5 min after reduction and most intense 1 day after reduction. Fluorescence spectra for these two extreme cases are shown in Figure 3A.

The corresponding raw mass spectra are shown in Figure 3B. All prominent $\text{Ag}_n\text{:DNA}$ peaks display adducts corresponding different numbers of bound Na^+ ions. The m/z spacing of these adducts allows unambiguous assignment of the charge state, z , of the peak. This z assignment is important for proper assignment of the $\text{Ag}_n\text{:DNA}$ peaks, as peaks with different n and different z can have similar m/z values (Supporting Information). The signal is strongest for $\text{Ag}_n\text{:DNA}$ with $z = 4–6$. We restrict our analysis to the m/z window displayed in Figure 3B, in which we identify only $z = 5$ species of $\text{Ag}_n\text{:DNA}$ with $n = 0–14$. Other peaks with more than 14 Ag may also be present in small amounts, but cannot be identified due to overlap with peaks from neighboring z values. Additionally, some peaks corresponding to m/z values of $\text{Ag}_n\text{:DNA}$ within the range $n = 0–14$, whose amplitudes were below the detection threshold for which z values could be unambiguously determined, were omitted from analysis ($n = 4, 5, 7–10$).

Red (560 nm, 620 nm) fluorescence intensity correlated well with mass abundance of $\text{Ag}_{13}\text{:DNA}$. Green (400 nm, 525 nm) fluorescence correlated well with mass abundance of $\text{Ag}_{11}\text{:DNA}$

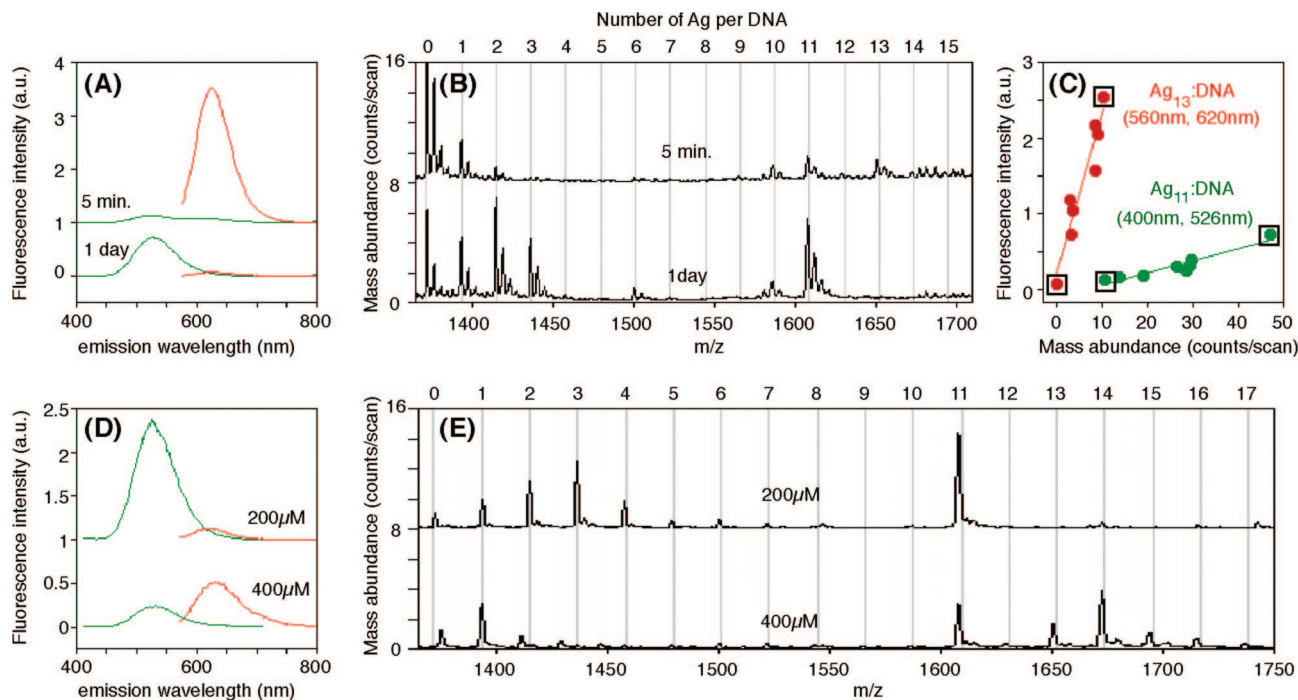


Figure 3. Corresponding fluorescence and mass spectroscopy of Ag clusters on 9C hairpins. (A–C) Ag clusters frozen at different times after reduction and measured immediately upon thawing. Red fluorescence dominates after 5 min; green fluorescence dominates after 1 day (A). Raw data for the corresponding mass spectra are shown over the m/z region corresponding to DNA + n Ag with $z = 5$, $n = 0–14$ (B). Comparison of mass abundance and fluorescence intensity reveals correlations between Ag_{11} :DNA and green emission as well as Ag_{13} :DNA and red emission (C). Black squares in (C) mark data points corresponding to 5 min and 1 day after reduction. Ag_2 :DNA and Ag_3 :DNA exhibited similar correlations with the green emission, but measurements under different synthesis conditions indicate that Ag_{11} :DNA best correlates with green fluorescence (D and E). Both 200 and 400 μM Ag solutions produce green fluorescence and Ag_{11} :DNA signal, but the signal for Ag_2 :DNA and Ag_3 :DNA drops below our detection threshold in the 400 μM Ag solution. (Low m/z peaks in the 400 μM spectrum correspond to $z = 4$, $n = 13–16$).

(Figure 3C). Green fluorescence also correlated with Ag_2 :DNA and Ag_3 :DNA for these 8 samples, so we performed a second set of fluorescence and mass spectroscopy measurements, which ruled out the Ag_2 :DNA and Ag_3 :DNA species as green emitters (Figure 3D,E). For this set of measurements, we synthesized 9C hairpin Ag clusters in 40 mM ammonium acetate using 25 μM DNA, 325 μM NaBH_4 , and 200 or 400 μM AgNO_3 . One week after reduction, we dialyzed them for 12 h in 2 L of 40 mM ammonium acetate using 3500 MWCO membranes. Both of these samples produced green fluorescence and Ag_{11} :DNA mass signal, but the 400 μM sample did not produce Ag_2 :DNA or Ag_3 :DNA above the detection threshold.

For a given emitter, fluorescence and mass abundance trends should be consistent with photophysical properties (extinction coefficient and quantum yield (QY)). We therefore set out to measure the absorbance and quantum yield (QY) of the 9C hairpin emitters. The presence of nonemissive absorbers at wavelengths near the red excitation peak prohibits a quantum yield measurement of the red emitter. We were however able to determine that the 9C green emitter has $\sim 3\%$ QY (Supporting Information). Measurements of extinction coefficients require more sophisticated experiments, and have not been performed here.

Dickson et. al report $\sim 32\%$ QY for a red emitter with spectra similar to that of our 9C hairpin clusters,¹³ suggesting that the 9C red emitter and the 9C green emitter may have QY's that differ by a factor of ~ 11 . We note that the slopes of the linear fits in Figure 3C differ by a factor of ~ 13 . The latter factor depends on the relative QYs and extinction coefficients of the emitters, as well as their relative detection efficiency by mass spectroscopy. We do not yet know the extinction coefficients, and the mass spectroscopy detection efficiencies depend on the

electrospray ionization process and are probably impossible to predict, but it is noteworthy that agreement of the above factors (~ 11 and ~ 13) does not require assumptions of dramatically different extinction coefficients or detection efficiencies.

The integrated fluorescence from the 9C green emitter in the 1 day sample (Figure 3A) is comparable to that of ~ 270 nM fluorescein (pH 7.5). This information can be combined with relative QYs and extinction coefficients of the green emitter and fluorescein to estimate the concentration of green clusters, and thus the fraction of DNA strands bound to green clusters. We measured $\text{QY}(\text{green cluster})/\text{QY}(\text{fluorescein pH 7.5}) = 3.7\%$. For lack of a measured extinction coefficient, we assume one equal to that of fluorescein, and estimate that green clusters bind $\sim 29\%$ of the DNA. (Dickson et al. reported extinction coefficients for yellow, red, and NIR DNA bound Ag clusters, ranging from ~ 1.5 to ~ 4.5 times that of fluorescein¹³). This rough estimate is consistent with an abundance of fluorescent species that is detectable by mass spectroscopy.

Conclusion

In conclusion, we have shown that DNA hairpins with poly-C loops stabilize four different types of fluorescent Ag clusters. We identified these four groups based on their peak wavelengths and stability. The physical features responsible for the grouping are yet to be determined. However, for the case of the 9C hairpin, fluorescence intensity and mass abundance correlate well for red emission and Ag_{13} :DNA, and for green emission and Ag_{11} :DNA, consistent with the possibility that the grouping represents clusters with different numbers of atoms. Notably, these cluster sizes are significantly larger than any previously suggested for DNA-bound Ag clusters with similar fluorescence.¹³

Our current efforts aim at identifying the composition of fluorescent species from the other DNA hairpins to obtain a more complete understanding of the emitter grouping. The mass spectra of other hairpins are more complex than that of the 9C hairpin, with broader distributions of cluster sizes. Identifying the fluorescent species in these solutions will require comparisons across a greater number of synthesis conditions or, even better, purification of the fluorescent species. Purification would also enable further characterization of the DNA-bound Ag clusters, using techniques such as NMR or X-ray scattering, that are not selective for fluorescent species.

Acknowledgment. We thank Steven K. Buratto for use of a scanning confocal microscope for spectroscopy of PVA embedded clusters. This work was supported by the National Science Foundation (CCF-0622257), a GK-12 Fellowship (NSF DGE-0440576) (P.O.), a GAANN Fellowship (DoE P200A060024) (P.O.), an Agilent Foundation Grant (07Q3-134FD) (L.V), and LSAMP program of the National Science Foundation (DMR-0611539) (L.V.).

Supporting Information Available: Quantum yield measurements, quantification of fluorescence, and mass abundance. This material is available free of charge via the Internet at <http://pubs.acs.org>.

References and Notes

- (1) Zheng, J.; et al. *Annu. Rev. Phys. Chem.* **2007**, *58*, 409.
- (2) Petty, J. T.; et al. *J. Am. Chem. Soc.* **2004**, *126*, 5207.
- (3) Vosch, T.; et al. *Proc. Natl. Acad. Sci. U.S.A.* **2007**, *104*, 12616.
- (4) Gwinn, E. G.; et al. *Adv. Mater.* **2008**, *20*, 279.
- (5) Rothmund, P. W. K. *Nature* **2006**, *440*, 297.
- (6) Seeman, N. C. *Mol. Biotechnol.* **2007**, *3*, 246.
- (7) Hettich, C.; et al. *Science* **2002**, *298*, 385.
- (8) Calarco, T.; et al. *Phys. Rev. A* **2003**, *68*, 012310.
- (9) Conus, F.; et al. *J. Chem. Phys.* **2006**, *125*, 024511.
- (10) Sun, T.; Seff, K. *Chem. Rev.* **1994**, *94*, 857.
- (11) Zheng, J.; Dickson, R. M. *J. Am. Chem. Soc.* **2002**, *124*, 13982.
- (12) Yu, J.; et al. *Angew. Chem., Int. Ed.* **2007**, *46*, 2028.
- (13) Richards, C. I.; et al. *J. Am. Chem. Soc.* **2008**, *130*, 5038.
- (14) The hairpins are predicted²⁴ to form in the absence of Ag⁺, which can mediate non-Watson–Crick base pairing²⁵.
- (15) Izatt, R. M.; et al. *Chem. Rev.* **1971**, *71*, 439.
- (16) Weston, K. D.; et al. *J. Chem. Phys.* **1998**, *109*, 7474.
- (17) Ritchie, C. M.; et al. *J. Phys. Chem. C* **2007**, *111*, 175.
- (18) Bonacic-Koutecky, V.; et al. *J. Chem. Phys.* **1999**, *110*, 3876.
- (19) Jensen, L.; et al. *J. Phys. Chem. C* **2007**, *111*, 4756–4764.
- (20) Fedrigo, S.; et al. *J. Chem. Phys.* **1993**, *99* (8), 5712.
- (21) Félix, C.; et al. *Chem. Phys. Lett.* **1999**, *313*, 105.
- (22) Félix, C.; et al. *Phys. Rev. Lett.* **2001**, *86*, 2992.
- (23) Sieber, C.; et al. *Phys. Rev. A* **2004**, *70*, 041201(R).
- (24) Owczarzy, R.; et al. *Nucleic Acids Res.* **2008**, *36*, W163.
- (25) Menzer, S.; et al. *J. Am. Chem. Soc.* **1992**, *114*, 4644.

JP809274M